Commun. Korean Math. Soc. **17** (2002), No. 1, pp. 103–120

A SECOND ORDER UPWIND METHOD FOR LINEAR HYPERBOLIC SYSTEMS

SUNG-IK SOHN AND JUN YONG SHIN

ABSTRACT. A second order upwind method for linear hyperbolic systems is studied in this paper. The method approximates solutions as piecewise linear functions, and state variables and slopes of the linear functions for next time step are computed separately. We present a new method for the computation of slopes, derived from an upwinding difference for a derivative. For nonoscillatory solutions, a monotonicity algorithm is also proposed by modifying an existing algorithm. To validate our second order upwind method, numerical results for linear advection equations and linear systems for elastic and acoustic waves are given.

1. Introduction

We consider the linear system of partial differential equations

$$U_t(x,t) + A\,U_x(x,t) = 0, \qquad (1)$$
$$U(x,t) = U_0(x),$$

where $U : R \times R \to R^m$ and $A \in R^{m\times m}$ is a constant matrix. This system is called *hyperbolic* if A is diagonalizable with real eigenvalues [1]. Moreover, if the eigenvalues are distinct, the system is called *strictly hyperbolic.* Many physical phenomena such as acoustics, elasticity, electromagnetics, and medical imaging are governed by the linear system (1). In this paper, we study numerical methods for solutions of strictly hyperbolic linear systems.

The methods studied here are upwind schemes. Upwind schemes are usually referred as the numerical methods taking into account upwind directions from which characteristic informations propagates [1]. Many

Received January 3, 2001.
2000 Mathematics Subject Classification: 65M06, 65M25.
Key words and phrases: upwind method, linear hyperbolic systems, slope limiter.
This work was supported by Korea Research Foundation Grant (KRF-99-015-DI0013).

high resolution upwind schemes for hyperbolic systems employ the Godunov method [2]. The Godunov method approximates the solutions as piecewise constant functions and is only first order accurate. For extension of the Godunov method to higher order accuracy, dominant approaches are the approximation of solutions as piecewise polynomials. The higher order upwind methods using piecewise polynomials have been successfully developed for nonlinear hyperbolic problems [3, 4, 5]. However, numerical methods of linear hyperbolic systems have their own importance and have been remained for improvements, as pointed out by Roe [6].

In this paper, we present a second order upwind method for linear hyperbolic systems, using piecewise linear polynomials. Such method was first studied by Van Leer [7] for the scalar advection equation. The Van Leer's method consists of two schemes, scheme for state variables and one for slopes of piecewise linear polynomials. Van Leer proposed three different methods for the computation of slopes. In addition to Van Leer's methods, we propose a new method for the slope computations.

Numerical solutions of higher order methods have oscillations around discontinuities and monotonicity of initial data is not preserved during the computation. Godunov proved that a linear monotonicity preserving method is at most first order accurate [2]. In the second order upwind methods, nonoscillatory solutions can be obtained by adjusting the slopes. Such adjusting algorithm is called the monotonicity algorithm or slope limiter. Among various choice of slope limiters, the algorithm proposed by Van Leer [7] is applied to our second order upwind method. We will show that the Van Leer's limiter works for most of linear systems, but for some linear systems, does not provide satisfactory monotonic solutions. Therefore, to overcome this situations, we propose a modified slope limiter, adjusting the Van Leer's limiter.

In Section 2, our second order upwind method is first derived for the scalar advection equation. Section 2 also gives the analysis of dissipation error of the method and the monotonicity algorithms. In Section 3, the second order upwind method constructed in Section 2 for the scalar case is generalized to linear hyperbolic systems and applied to elastic and acoustic wave equations. Section 4 gives results of numerical experiments for the linear advection equation, and the elastic and acoustic wave equation.

2. Scalar advection equation

2.1. Second order method

We first consider the scalar linear advection equation

$$u_t + au_x = 0, \qquad a > 0. \tag{2}$$

We discretize the $x - t$ plane by a mesh width $h \equiv \Delta x$ and a time step $k \equiv \Delta t$, and use j and n for the index of discrete mesh points of space and time, respectively.

The initial data at each time level is approximated as a piecewise linear polynomial. We denote the pointwise approximate values of the state variables by $u_j^n = u(x_j, t_n)$ and ones for slopes by $\Delta u_j^n / h = u_x(x_j, t_n)$. Then, at each mesh, we may write

$$u(x,t) = u_j + \frac{\Delta u_j}{h}(x - x_j), \quad x_{j-1/2} < x < x_{j+1/2}. \tag{3}$$

Here $x_{j+1/2}$ is the midpoint of x_j and x_{j+1}, and is called the edge of mesh. To derive the second order method, we use Taylor series in time for $u(x, t+k)$.

$$u(x,t+k) = u(x,t) + ku_t(x,t) + \frac{k^2}{2}u_{tt}(x,t) + O(k^3). \tag{4}$$

Applying (2) to (4), we have

$$u(x,t+k) = u(x,t) - aku_x(x,t) + \frac{a^2k^2}{2}u_{xx}(x,t) + O(k^3). \tag{5}$$

Replacing the derivatives in x by a finite difference to the upwind direction (upwind difference) and applying Taylor series,

$$\begin{aligned} u(x,t+k) &= u(x,t) - \frac{ak}{h}(u(x,t) - u(x-h,t)) \\ &\quad - \frac{ak}{2}(1 - \frac{ak}{h})(u_x(x,t) - u_x(x-h,t)) \\ &\quad + O(k^2h) + O(kh^2) + O(k^3). \end{aligned} \tag{6}$$

Then, (6) gives the method for state variables

$$u_j^{n+1} = u_j^n - \nu(u_j^n - u_{j-1}^n) - \frac{1}{2}\nu(1-\nu)(\Delta u_j^n - \Delta u_{j-1}^n), \tag{7}$$

where ν is the Courant-Friedrichs-Lewy (CFL) number

$$\nu = \frac{ak}{h}. \tag{8}$$

For stability, ν should satisfy the CFL condition

$$|\nu| = |a|\frac{k}{h} \leq 1. \tag{9}$$

It is seen that the method (7) is the result of a first order upwind method

$$u_j^{n+1} = u_j^n - \nu(u_j^n - u_{j-1}^n) \tag{10}$$

with a second order correction term

$$-\frac{1}{2}\nu(1-\nu)(\Delta u_j^n - \Delta u_{j-1}^n) \tag{11}$$

added.

(7) has the same form as equation (14) in Van Leer [7]. However, eq. (14) in [7] is for the mesh average of state variables, while (7) is directly for the state variables.

Now the question is how we choose the gradient Δu. The accuracy of the method (7) depends on the extra scheme for Δu.

Van Leer [7] proposed three methods to determine Δu, which are based on the central difference of neighboring nodes, the central difference of neighboring edges, and the first moment of state variables in mesh. It was shown that the third one, based on the first moment of state variables, was best in accuracy and stability. We denote this method as VL^3. Since VL^3 is related to our new method, we rewrite the expression here

$$\begin{aligned} \bar{\Delta} u_j^{n+1} &= 6\nu(1-\nu)(\bar{u}_j^n - \bar{u}_{j-1}^n) + (1-\nu)(1-2\nu-2\nu^2)\bar{\Delta} u_j^n \\ &\quad - \nu(3-6\nu+2\nu^2)\bar{\Delta} u_{j-1}^n, \end{aligned} \tag{12}$$

where the bar means the mesh average. It is interesting that, for the scalar advection equation, the method (7) and (12) are the same as the discontinuous Galerkin method [8], although the approaches of the two methods are different.

In VL^3, to obtain the first moment of solutions, the full analytic solutions at next time step should be known from the characteristics. If this approach is applied to nonlinear hyperbolic equations, it becomes very complicated, so that it is rarely used in nonlinear equations. Here we derive a new and simple method for the gradient Δu from an upwind difference for the derivative, not by using the full analytic solutions.

To determine Δu, we apply the similar approach as the derivation of (7). Applying Taylor series for $u_x(x, t+k)$ in time and equation (2), it gives

$$u_x(x,t+k) = u_x(x,t) - aku_{xx}(x,t) + \frac{a^2k^2}{2}u_{xxx}(x,t) + O(k^3). \tag{13}$$

Replacing $u_x(x,t)$ by the upwind difference and applying Taylor series,

$$\begin{aligned} u_x(x,t+k) &= u_x(x,t) - \frac{ak}{h}(u_x(x,t) - u_x(x-h,t)) \\ &\quad + \frac{ak}{2}(ak-h)u_{xxx}(x,t) + O(kh^2) + O(k^3). \end{aligned} \tag{14}$$

One can easily show that $u_{xxx}(x,t)$ is approximated as

$$\begin{aligned} u_{xxx}(x,t) &= -\frac{12}{h^3}(u(x,t) - u(x-h,t)) \\ &\quad + \frac{6}{h^2}(u_x(x,t) + u_x(x-h,t)) + O(h). \end{aligned} \tag{15}$$

Substituting (15) into (14), we obtain

$$\begin{aligned} u_x(x,t+k) &= u_x(x,t) + 6\frac{ak}{h^2}(1 - \frac{ak}{h})(u(x,t) - u(x-h,t)) \\ &\quad - \frac{ak}{h}(4 - 3\frac{ak}{h})u_x(x,t) - \frac{ak}{h}(2 - 3\frac{ak}{h})u_x(x-h,t) \\ &\quad + O(k^2h) + O(kh^2) + O(k^3). \end{aligned} \tag{16}$$

This gives the method for the gradients

$$\begin{aligned} \Delta u_j^{n+1} &= \Delta u_j^n + 6\nu(1-\nu)(u_j^n - u_{j-1}^n) \\ &\quad - \nu(4-3\nu)\Delta u_j^n - \nu(2-3\nu)\Delta u_{j-1}^n. \end{aligned} \tag{17}$$

Equations (7) and (17) form the full method. It is obvious from (6) and (16) that the method (7) and (17) are second order accurate. We note that the expression of (17) differs with VL^3 in the coefficients of Δu_j^n and Δu_{j-1}^n. We note that, for $\nu = 1/2$, (17) becomes identical to VL^3.

The matrix form of the method (7) and (17) is

$$\begin{pmatrix} u \\ \Delta u \end{pmatrix}_j^{n+1} = ((1-\nu)A + \nu T^{-1}B)\begin{pmatrix} u \\ \Delta u \end{pmatrix}_j^n, \tag{18}$$

where

$$A = \begin{pmatrix} 1 & -\frac{1}{2}\nu \\ 6\nu & 1-3\nu \end{pmatrix}, \quad B = \begin{pmatrix} 1 & \frac{1}{2}(1-\nu) \\ 6(\nu-1) & -2+3\nu \end{pmatrix}$$

and T denotes a space translation over h.

So far we assumed $a > 0$. A similar method can be defined for $a < 0$. To extend the method to linear systems at Section 3, we need to express the method for arbitrary wave speeds. The general formulations of (7) and (17) for arbitrary wave speeds are

$$u_j^{n+1} = u_j^n - \nu(u_{j_1}^n - u_{j_1-1}^n) - \frac{1}{2}\nu(\mathrm{sgn}(\nu) - \nu)(\Delta u_{j_1}^n - \Delta u_{j_1-1}^n) \tag{19}$$

and

$$\begin{aligned} \Delta u_j^{n+1} &= \Delta u_j^n + 6\nu(\mathrm{sgn}(\nu) - \nu)(u_{j_1}^n - u_{j_1-1}^n) \\ &\quad - \nu(4\,\mathrm{sgn}(\nu) - 3\nu)\Delta u_{j_1}^n - \nu(2\,\mathrm{sgn}(\nu) - 3\nu)\Delta u_{j_1-1}^n, \end{aligned} \tag{20}$$

where

$$j_1 = \begin{cases} j & \text{if } a > 0 \\ j+1 & \text{if } a < 0. \end{cases} \tag{21}$$

2.2. Analysis for dissipation

In this section, we analyze the dissipation error of the second order upwind method and compare with the Van Leer's method. We assume oscillatory initial data

$$u_j^n = g^n e^{ij\theta}. \tag{22}$$

Then, the translation operator is

$$T = e^{i\theta}. \tag{23}$$

The amplification factor g in our case are eigenvalues of the matrix $(1-\nu)A + \nu T^{-1}B$ in (18). Therefore, by substituting (23) into the matrix of (18), one can obtain the amplification factor for the second order upwind method

$$\begin{aligned} g = e^{-i\theta/2}\Big[& (1 - 3\nu + 3\nu^2)\cos(\theta/2) + \mathrm{i}(1 - 2\nu)\sin(\theta/2) \\ & \pm \Big\{\frac{21}{2}\nu^2(1-\nu)^2 - \frac{3}{2}\nu^2(1-\nu)^2\cos\theta \\ & + \mathrm{i}(1 - 3\nu + 3\nu^2)(\nu - \frac{1}{2})\sin\theta\Big\}^{1/2}\Big]. \end{aligned} \tag{24}$$

Equation (24) satisfies

$$g(1-\nu) = e^{-i\theta} g^*(\nu), \tag{25}$$

where the star denotes the complex conjugate. Then, from (25) the symmetry relations hold

$$|g(1-\nu)| = |g(\nu)|, \tag{26}$$

$$\arg g(1-\nu) + (1-\nu)\theta = -\{\arg g(\nu) + \nu\theta\}. \tag{27}$$

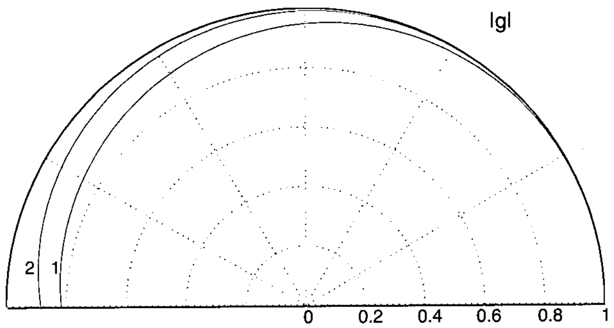

FIGURE 1. Polar plot of the radius of amplification factor $|g|$ as a function of wave number θ for CFL number 0.8. The curve 1 corresponds to the second order upwind method and the curve 2 for VL^3.

Van Leer showed that the three methods proposed in [7] also satisfied the symmetry relations (26) and (27), and compared the accuracy for $\nu = 1/2$, since the methods have a maximum dissipation error and a zero phase error at $\nu = 1/2$ by the symmetry relations. Since our second order upwind method and the Van Leer's third method (VL^3) are identical for $\nu = 1/2$, the analysis given in [7] is equally applicable to our method. Here we compare the dissipation error of our method with VL^3 for $\nu = 0.8$. Note that the CFL number between 1/2 and 1 is widely used for linear hyperbolic systems.

Figure 1 is the polar plot of the radius of amplification factor as a function of the wave number θ for our second order upwind method and VL^3 for $\nu = 0.8$. Figure 1 shows that the dissipation error per time step, $1-|g(\nu)|$, of our second order upwind method is slightly larger than that of VL^3. However, the differences of error of the two methods are small and the qualitative behaviors of dissipations are similar.

2.3. Monotonicity algorithms

It is well known that second order methods for hyperbolic systems suffer from oscillations around discontinuities [1]. Various methods, such as artificial viscosity and total variation diminishing (TVD) methods, have been developed to overcome this difficulty [1, 9, 10]. Van Leer [7] also proposed monotonicity algorithms, which says that, when a monotonic initial value distribution is numerically convected, the resulting distribution remains monotonic.

Among the several monotonicity algorithms proposed by Van Leer, the suitable choice for our problem is

(28)

$$(\Delta u_j)\text{mono} = \begin{cases} \min\{2|u_{j+1} - u_j|,\ |\Delta u_j|,\ 2|u_j - u_{j-1}|\}\ \text{sgn}(\Delta u_j) \\ \qquad \text{if } \text{sgn}(u_{j+1} - u_j) = \text{sgn}(\Delta u_j) = \text{sgn}(u_j - u_{j-1}), \\ 0 \qquad \text{otherwise.} \end{cases}$$

Δu_j computed by (20) is adjusted by (28). Therefore, the monotonicity algorithm is often called as the slope limiter.

(28) was derived by giving the condition that the linear function (3) should not take values outside the range spanned by the neighboring mesh averages. The slope limiter (28) provides a sharp resolution around a shock and works for most of problems. However, the limiting is too strong and gives slight oscillations in some cases. Van Leer proposed another slope limiter, which is a function of the CFL number, to remedy this trouble. However, that slope limiter has a complicated expression. Therefore, we propose a modified slope limiter, by reducing the factor 2 in (28) to 1,

(29)

$$(\Delta u_j)_{\text{mod}} = \begin{cases} \min\{|u_{j+1} - u_j|,\ |\Delta u_j|,\ |u_j - u_{j-1}|\}\ \text{sgn}(\Delta u_j) \\ \qquad \text{if } \text{sgn}(u_{j+1} - u_j) = \text{sgn}(\Delta u_j) = \text{sgn}(u_j - u_{j-1}), \\ 0 \qquad \text{otherwise.} \end{cases}$$

The limiter (28) and (29) can be derived from the concept of TVD. In fact, the monotonicity algorithm is mathematically equivalent to the TVD method. Recently we have derived the second order TVD region of the upwind methods using a piecewise linear polynomial. This results will be published elsewhere. The limiter (28) and (29) correspond to different boundaries of the second order TVD region of the upwind methods.

The limiter (29) still guarantees the second order accuracy of the upwind method (19) and (20). The first choice in the bracket of min in (29) gives the Lax-Wendroff method, while the third choice gives the Beam-Warming method [1]. We will show at the numerical example that the limiter (29) mush be used in some cases instead of (28). We can also expect that, by using the modified slope limiter, the resolution will be slightly reduced, since the factor 2 in (28) has the effect of steepening the profile.

3. Linear systems

3.1. General formulations

The method (19) and (20) for the scalar advection equation can be generalized for linear systems (1) by diagonalizing the matrix and applying the method of the previous section to each decoupled scalar problem.

Since the matrix A in (1) is diagonalizable by the definition, we can decompose

$$A = R\Lambda R^{-1}, \tag{30}$$

where $\Lambda = \text{diag}(\lambda_1, \lambda_2, .., \lambda_m)$ is a diagonal matrix of eigenvalues and $R = [r_1|r_2|\cdots|r_m]$ is the matrix of right eigenvectors. We let

$$W_j^n = R^{-1}U_j^n \tag{31}$$

and W_j^n have components W_{pj} so that $U_j^n = \sum_{p=1}^m W_{pj}r_p$, where r_p is the p-th eigenvector. We also set

$$j_p = \begin{cases} j & \text{if } \lambda_p > 0 \\ j+1 & \text{if } \lambda_p < 0 \end{cases} \tag{32}$$

generalizing j_1 defined in (21). Then, the method (19) for each W_{pj} takes the form

$$\begin{aligned} W_{pj}^{n+1} &= W_{pj} - \nu_p(W_{pj_p} - W_{p,j_p-1}) \\ &\quad -\frac{1}{2}\nu_p(\text{sgn}(\nu_p) - \nu_p)(\Delta W_{pj_p} - \Delta W_{p,j_p-1}), \end{aligned} \tag{33}$$

where $\nu_p = k\lambda_p/h$. Multiplying (33) by r_p and summing over p,

$$\begin{aligned} U_j^{n+1} &= \sum_{p=1}^m W_{pj}^{n+1} r_p \\ &= U_j^n - \sum_{p=1}^m \nu_p(W_{pj_p} - W_{p,j_p-1})r_p \\ &\quad - \frac{1}{2}\sum_{p=1}^m \nu_p(\text{sgn}(\nu_p) - \nu_p)(\Delta W_{pj_p} - \Delta W_{p,j_p-1})r_p. \end{aligned} \tag{34}$$

Similarly, the method (20) for gradients can be generalized for the system and the resulting form is

$$\begin{aligned}\Delta U_j^{n+1} \;=\; & \Delta U_j^n + 6\sum_{p=1}^{m} \nu_p(\operatorname{sgn}(\nu_p) - \nu_p)(W_{pj_p} - W_{p,j_p-1})r_p \\ & - \sum_{p=1}^{m} \nu_p \left[(4\operatorname{sgn}(\nu_p) - 3\nu_p)\Delta W_{pj_p}\right. \\ & \left. + (2\operatorname{sgn}(\nu_p) - 3\nu_p)\Delta W_{p,j_p-1})\right] r_p. \end{aligned} \tag{35}$$

To remove the oscillations around the discontinuities, the monotonicity algorithms discussed in the last section should be applied to each component of ΔU_j.

3.2. Elastic and acoustic wave equations

We take the elastic and acoustic wave equations for illustrative examples of linear hyperbolic systems. To apply the upwind method described at the last section, all we have to do is finding eigenvalues and eigenvectors of the matrix in governing equations.

EXAMPLE 1 (Elastic wave). Consider an isotropic elastic medium undergoing small transient displacements. There are many ways to write the governing equation as a first order system, according to the choice of dependent variables. Here we choose $U = (u, \epsilon)^T$, where u is the particle velocity and ϵ the strain. Then, the matrix of the linear system (1) is

$$A = \begin{pmatrix} 0 & -E/\rho \\ -1 & 0 \end{pmatrix}, \tag{36}$$

where ρ is the density of the medium. E is Young's modulus from the Hookes's law $\sigma = E\epsilon$, where σ is the stress. The eigenvalues of A are $\lambda = \pm\sqrt{E/\rho}$ and the corresponding eigenvectors are $(\sqrt{E/\rho}, \pm 1)$.

EXAMPLE 2 (Acoustic wave). The governing equation for acoustic waves in a uniform medium can be written in the form (1) with variables $U = (u, p)^T$, where u is the particle velocity and p the pressure. The matrix is

$$A = \begin{pmatrix} 0 & 1/\rho \\ \rho c^2 & 0 \end{pmatrix}, \tag{37}$$

where ρ is the density, and c the sound speed of the medium. The eigenvalues of A are $\lambda = \pm c$ and the corresponding eigenvectors are $(1, \pm\rho c)$.

4. Numerical Results

In this section, we perform numerical tests for the scalar advection equation, and the elastic and acoustic wave equations to demonstrate the validity of our second order upwind method. The CFL numbers are set to 0.8 through all numerical tests given in this section.

The second order upwind method is first applied to the scalar advection equation (2) with $a = 1$. The initial data is a square wave

$$u(x, t = 0) = \begin{cases} 0.5 & \text{if } -0.5 < x < 0 \\ 0 & \text{otherwise.} \end{cases}$$

The square wave is discretized by 25 grid points with spacing $h = 0.02$. Figure 2 and 3 display numerical solutions at time $t = 0.496$ obtained from the first order upwind method (10) and the Lax-Wendroff method, respectively. The exact solutions are shown by full lines for comparison. The first order results in Figure 2 are inaccurate throughout and the discontinuities are smeared by diffusion. Figure 3 shows that the second order results of the Lax-Wendroff method help to sharpen steep gradients but introduce large spurious oscillations.

Figure 4 shows numerical solutions, at the same time t as Figure 2 and 3, obtained from the second order upwind method (19) and (20) without/with using the slope limiter (28). Figure 4(a) shows that the results of the second order upwind method have steep gradients and also have slight oscillations after shocks. It is found that the amplitude and width of oscillations of the second order upwind method are much smaller than that of the Lax-Wendroff method. Figure 4(b) shows that the second order upwind method with the slope limiter gives high resolutions around shocks without oscillations.

Now, we apply the second order upwind method (34) and (35) to the linear systems of the elastic wave. We assume $\rho = 1$ and $E = 1$, and consider again a square wave for initial data

$$\epsilon = -u = \begin{cases} 1 & \text{if } 0 < x < 1 \\ 0 & \text{otherwise.} \end{cases}$$

This square wave is an idealized model for an impact in an one-dimensional elasticity problem. The square wave is discretized by 25 grid points with spacing $h = 0.04$. Figure 5 displays numerical solutions of the strain at time $t = 0.992$ obtained by the second order upwind method (34) and (35) without/with the slope limiter (28). The behavior of solutions are similar to the scalar advection case and this result shows the validity of our upwind method for linear hyperbolic systems.

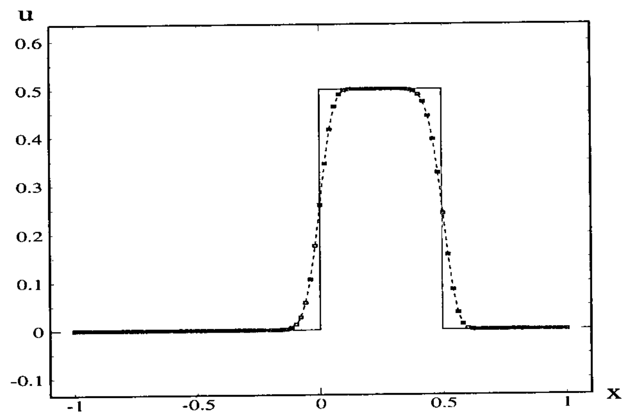

FIGURE 2. Solution of $u_t + u_x = 0$ by the first order upwind method. The initial data is a square wave. The numerical result is shown by symbols and the exact solution by full line.

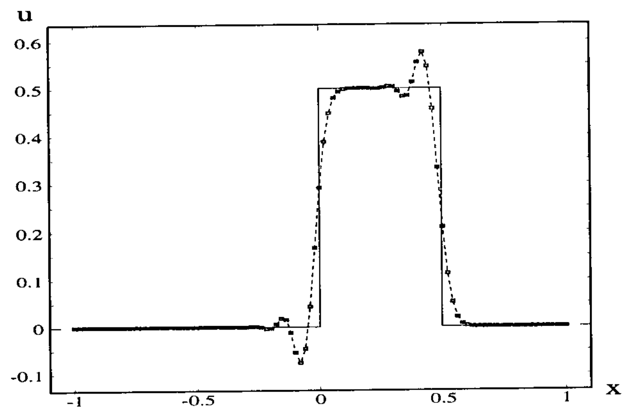

FIGURE 3. Solution of $u_t + u_x = 0$ by Lax-Wendroff method. The initial data is same as Figure 2. The numerical result is shown by symbols and the exact solution by full line.

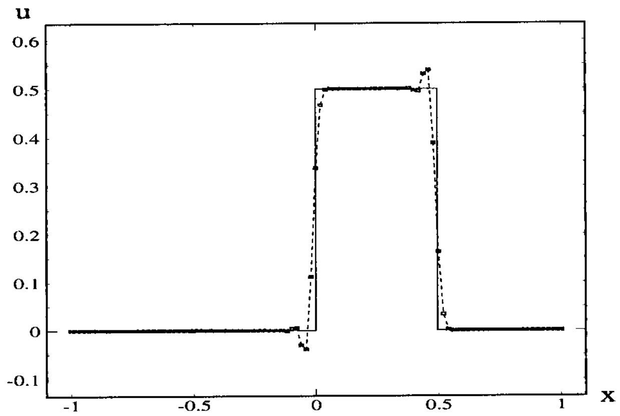

(a)

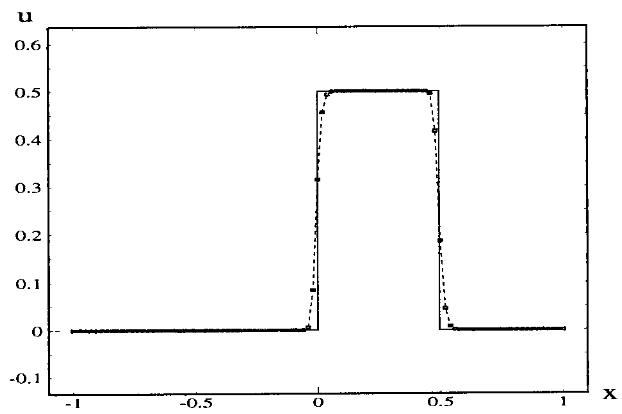

(b)

FIGURE 4. Solutions of $u_t + u_x = 0$ by the second order upwind method. (a) the result not using the slope limiter, (b) the result using the slope limiter. The initial data is same as Figure 2. The numerical results are shown by symbols and the exact solutions by full line.

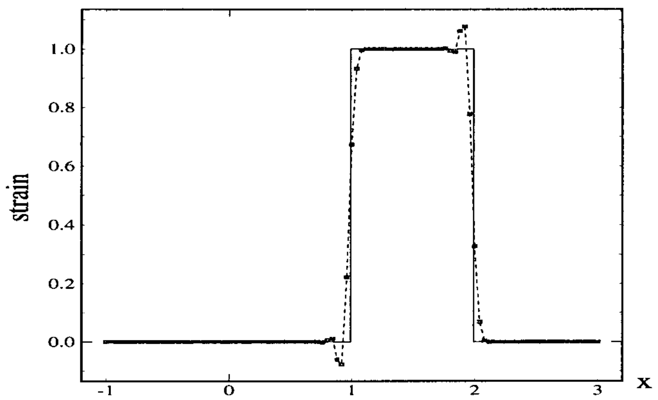

(a)

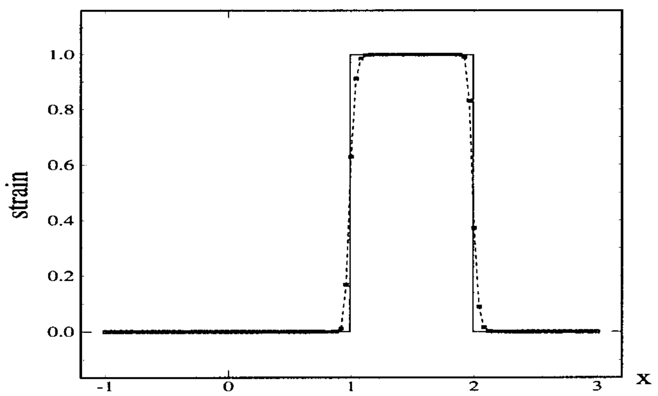

(b)

FIGURE 5. Solutions of the elastic wave equation by the second order upwind method. (a) the result not using slope limiter, (b) the result using slope limiter. The initial data is a square wave. The numerical results are shown by symbols and the exact solutions by full line.

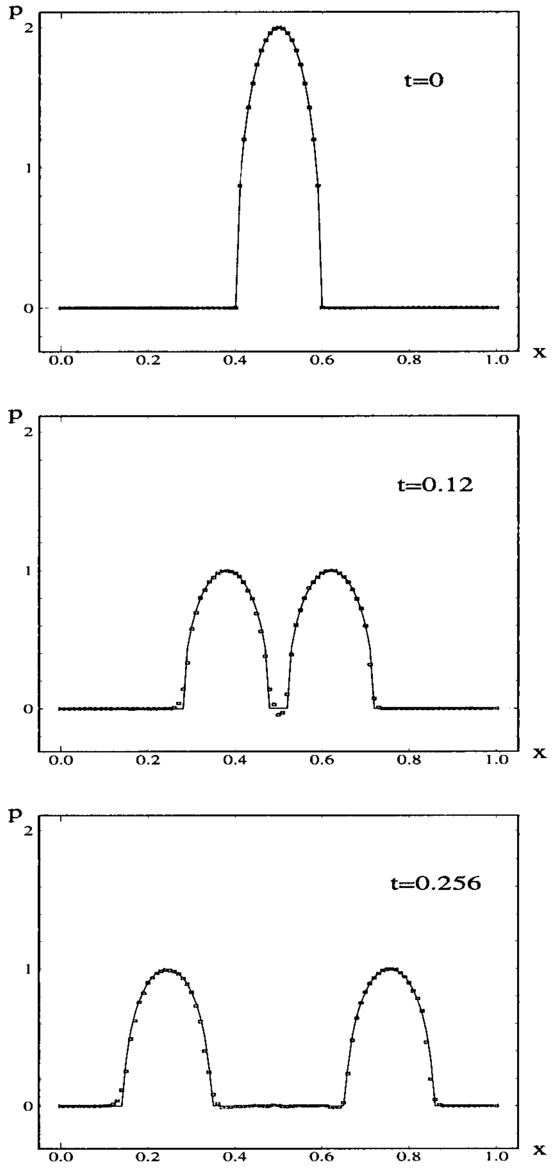

FIGURE 6. Solutions of the acoustic wave equation by the second order upwind method using the slope limiter (28). The numerical results are shown by symbols and the exact solutions by full line.

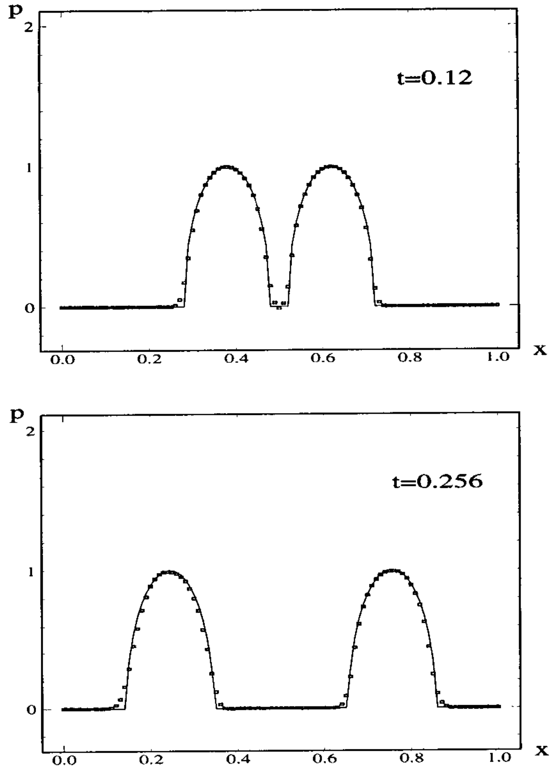

FIGURE 7. Solutions of the acoustic wave equation by the second order upwind method using the slope limiter (29). The initial data is same as Figure 6. The numerical results are shown by symbols and the exact solutions by full line.

Next, we consider the acoustic wave equation. We set $\rho = 1$ and $c = 1$. As initial data we take $u \equiv 0$ and a hump in pressure

$$p(x,0) = \begin{cases} \bar{p}\sqrt{1-((x-x_0)/\bar{x})^2} & \text{if } |x-x_0| < \bar{x} \\ 0 & \text{otherwise,} \end{cases}$$

with $x_0 = 0.5, \bar{x} = 0.1$, and $\bar{p} = 0.2$. The hump splits into equal left-going and right-going pieces. This is a nice test problem, since, when the hump is splitted, it has an infinite slope at the corners as well as the initial smoothness region. This initial data is a half ellipse of the type use in Zalesak [11]. Figure 6 shows the exact solutions and numerical solutions of the pressure at three different times obtained by the second order upwind method with the slope limiter (28). The computational domain $[-1, 1]$ is discretized by 100 grid points. We have checked that the second order upwind method without the slope limiter was crashed in the middle of computation due to oscillations. In Figure 6, overshoots are found just after the wave is splitted and this overshoots result in oscillatory solutions behind moving waves.

The overshoots and oscillations from the slope limiter (28) can be fixed by the modified slope limiter (29). Figure 7 is the results of the second order upwind method with the modified slope limiter (29). The initial conditions and numerical parameters of Figure 7 are the same as the ones in Figure 6. Using the modified limiter, the overshoots are much reduced and numerical solutions are monotonic and have no oscillation. One can also see that the diffusions at the corner of solutions of Figure 7 are slightly larger than that of Figure 6, as expected.

5. Conclusions

For the linear hyperbolic systems, the second order upwind methods using piecewise linear functions for the approximation of solutions were studied. We proposed a new method for computation of slopes of the linear functions and a modified slope limiter for monotonic profile of solutions. The analysis and numerical results showed that the new method equipped with a slope limiter provides the high resolution of solutions without oscillations and is comparable with the Van Leer's methods.

We also showed in the numerical results for the acoustic wave equation that the strong limiter may give overshoots and oscillatory solutions. Therefore, we conclude that the quality of solutions from a slope limiter depends on initial data and problems, so that the limiter should be carefully chosen.

Our second order method based on the piecewise linear functions can be naturally extended to a third order method using the piecewise quadratic functions. Our results presented in this paper show that the numerical methods for linear hyperbolic systems are still remained for improvements in many features.

References

[1] R. J. LeVeque, *Numerical methods for conservation laws*, Birkhäuser, Basel, 1992.

[2] S. K. Godunov, *Difference methods for the numerical calculation of the equations of fluid dynamics*, Mat. Sb. **47** (1959), 271–290 (In Russian).
[3] B. V. Leer, *Towards the ultimate conservative difference method V. A second order sequel to Godunov's method*, J. Comput. Phys. **32** (1979), 101–136.
[4] P. Colella, *A direct Eulerian MUSCL scheme for gas dynamics*, SIAM J. Sci. Stat. Comput. **6** (1985), 104–117.
[5] A. Harten, B. Engquist, S. Osher, and S. Chakravarthy, *Uniformly high order accurate essentially nonoscillatory schemes III*, J. Comput. Phys. **71** (1987), 231–303.
[6] P. Roe, *Linear bicharacteristic schemes without dissipation*, SIAM J. Sci. Comput. **19** (1998), 1405–1427.
[7] B. V. Leer, *Towards the ultimate conservative difference method IV. A new approach to numerical convection*, J. Comput. Phys. **23** (1977), 276–299.
[8] C. Johnson and J. Pitkäranta, *An analysis of the discontinuous Galerkin method for a scalar hyperbolic equation*, Math. Comp. **46** (1986), 1–26.
[9] A. Harten, *High resolution methods for hyperbolic conservation laws*, J. Comput. Phys. **49** (1983), 357–393.
[10] P. K. Sweby, *High resolution methods using flux limiters for hyperbolic conservation laws*, SIAM J. Numer. Anal. **21** (1984), 995–1011.
[11] S. T. Zalesak, *A preliminary comparison of modern shock-capturing methods: linear advection*, Advances in Computer Methods for Partial Differential Equations VI, IMACS, Baltzer, Basel, 1987.

Sung-Ik Sohn
School of Information Engineering
Tongmyong University of Information Technology
535 Yongdang-dong
Pusan 608-711, Korea
E-mail: sohnsi@tmic.tit.ac.kr

Jun Yong Shin
Division of Mathematical Sciences
Pukyung National University
599-1 Daeyeon3-dong
Pusan 608-737, Korea
E-mail: jyshin@dolphin.pknu.ac.kr